

Mixed-Ligand Ni(II), Co(II) and Fe(II) Complexes as Catalysts for Esterification of Biomass-Derived Levulinic Acid with Polyol and *in Situ* Reduction via Hydrogenation with NaBH₄

Md. Anwar Hossain^{1,2} and Lee Hwei Voon^{1,*}

¹Nanotechnology & Catalysis Research Centre (NanoCat), Level 3, Block A, Institute of Postgraduate Studies, University of Malaya, Kuala Lumpur 50603, Malaysia.

²Department of Chemistry, Rajshahi University of Engineering & Technology, Rajshahi 6204, Bangladesh.

*Corresponding Author: Lee Hwei Voon. Email: leehweivoon@um.edu.my.

Abstract: Synthesizing polyol-based ester from biomass feedstocks for the preparation of biolubricant overcomes the dependence on petroleum oil usage. Albeit biomass-derived bio-oil is an alternative for the production of polyol ester, upgrading is essential prior to use as biolubricant. Levulinic acid (LA), obtained from bio-oil was applied for the catalytic esterification with two polyols, e.g., trimethylolpropane (TMP) and pentaerythritol (PE), in the presence of mixed-ligand Ni(II), Co(II), and Fe(II) complexes as catalyst. New mixed-ligand coordination complexes with empirical formula; [Ni(Phe)(Bpy)Cl].H₂O, [Co(Phe)(Bpy)Cl].H₂O, and [Fe(Phe)(Tyr)Cl].H₂O were synthesized by the reaction of ligands [L-phenylalanine (Phe), 4,4'-bipyridine (Bpy), and L-tyrosine (Tyr)] with metal chloride salts and characterized by elemental analysis, magnetic susceptibility, FTIR, TGA/DTA, powder-XRD, and SEM techniques. This study aims to investigate the catalytic activities of the complexes via esterification reaction of levulinic acid with trimethylolpropane and pentaerythritol. In addition, these catalysts were further employed for the *in situ* hydrogenation of levulinate esters via NaBH₄ at room temperature upon refluxing. Indeed, the iron(II) complex was more potential, exhibiting its efficiency as a homogeneous catalyst for esterification-hydrogenation reaction for synthesizing ester-based oils.

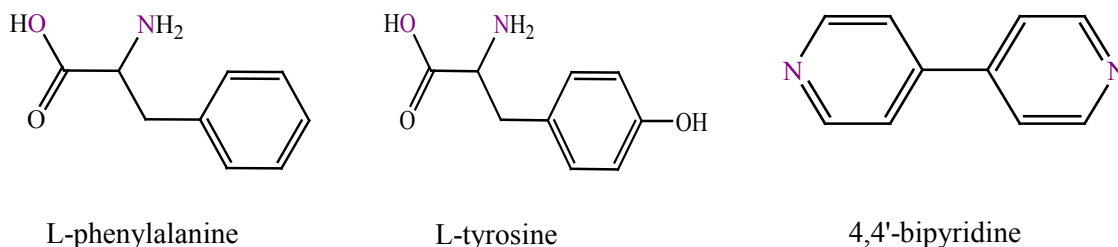
Keywords: Biomass; esterification-hydrogenation; mixed-ligand complex; NaBH₄; reduction

1 Introduction

Cheapest and efficient biomass conversion processes have recently been widely explored to overcome the global energy crisis [1-3]. Usage of biomass as a renewable resource to produce biolubricants and fine chemicals are the most important alternatives for current mineral oil-based technologies. Biomass (i.e., wood, corn, straw, soybean, grass, and algae), through pyrolysis or hydrotreating processes, produces various organic compounds, including biochar and bio-oil [4,5]. The bio-oil contains approximately 400 organic compounds, including carboxylic acids, e.g., acetic, propionic, and levulinic acid [6,7]. Levulinic acid (LA), having five carbon atoms with a carboxyl and ketone functional group, can also be derived from glucose, fructose, starch, and lignocellulosic residues [8,9]. This acid has been recognized by the U.S. Department of Energy as a top platform for chemicals, and is regarded as one of the 12 most attractive chemicals derived from wood-based feedstocks [10-12]. Levulinic acid can easily react with polyols, e.g., neopentyl glycol (NPG), trimethylolpropane (TMP), and pentaerythritol (PE), in the presence of acid catalysts via esterification reaction to give levulinate polyol esters [13]. These polyol ester base oils are used for lubricant formulation, plasticizers, fragrant chemicals,

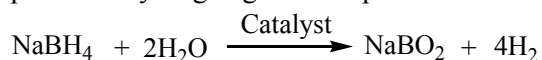
green solvents [14-16], and perfumery. In this study, TMP and PE levulinate esters are synthesized, for they are expected to have analogous lubricant properties to other polyol esters, having the same viscosity index, pour point, flash point, and biodegradability. Thus, there may be broader application sights for levulinic acid to produce biolubricants [16,17] compared to vegetable oils in economic perspectives.

Novel inorganic-organic hybrid complexes resulted as active areas of material science and chemical research, due to their ability to act as a catalyst or catalyst precursors. The thermal stability and tenability of metal-organic coordination complexes make them truly suitable for a wide range of catalytic and stoichiometric transformations. These comprise many reactions, including bond activation [18,19], carbon-carbon bond formation [20,21], polymerization [22], production of ammonia from nitrogen and hydrogen [23], organic synthesis [24,25], and supramolecular chemistry [26]. The donor atoms of employed mixed ligands for complex formation are depicted below (violet color):



Reduction plays an important role in various organic transformations. The reduction of esters to corresponding hydrocarbon based-esters is one of the most promising reactions in organic chemistry, and is, therefore, applied to a large number of chemical processes. Generally, there are two main ways to attain such a reduction [27] process by hydrogenation. Firstly, by using metal hydride salts (e.g., LiAlH_4 and NaBH_4), and the other is by using molecular hydrogen (H_2) in the reaction system. Lithium aluminum hydride (LiAlH_4) is a powerful reducing agent, thus its high reactivity has a disadvantage in most of the organic synthesis that cannot be used for selective reduction. By contrast, NaBH_4 is a less powerful reducing agent that is comparatively safe for the hydrogenation [28-32], even though it can be used in its solid form. Sodium borohydride is a commonly used reagent primarily for the selective reduction of carbonyl compounds [33,34], p-nitrophenol to p-aminophenol [35], while being combined with metal salts and various solvents which provide an excellent variety of reducing systems. Unlike LiAlH_4 , it can be used even in the aqueous or alcoholic solutions, and are safe, inexpensive, and environmentally friendly.

Recently, instead of using free hydrogen gas (i.e., traditional hydrogenation), the sources of hydrogen such as ammonia borane [36], dimethyl ammonia borane [37], liquid methanol [38], formic acid [39], and sodium borohydride [40-42] have been given preference. Of them, NaBH_4 is quite stable, cheaper, eco-friendly, and water soluble that can be used under mild reaction conditions. However, it produces hydrogen gas in the presence of catalyst-water system as follows [43,44]:



Herein, we report the synthesis of LA + TMP and LA + PE reduced esters by applying NaBH_4 in the presence of nickel(II), cobalt(II), and iron(II) complexes as catalyst under mild reaction conditions. The ester product and reduced ester products are finally characterized by GC-MS and FT-IR analysis.

2 Experimental

2.1 Materials

All the chemicals and solvents were of analytical grade and used without further purification. L-phenylalanine and L-tyrosine were obtained from Sigma-Aldrich (USA), while 4,4'-bipyridine was purchased from Merck (India). The metal salt Ni(II), Co(II), and Fe(II) chlorides were received from

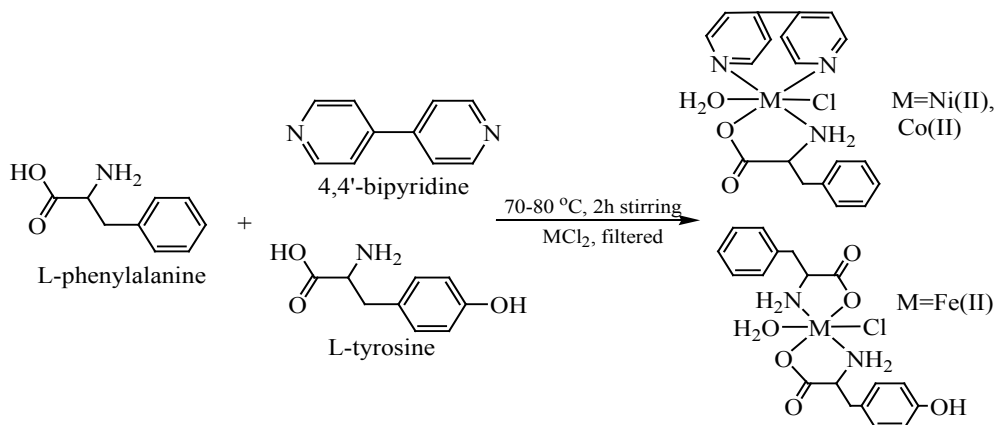
Fluka Chemica (Switzerland). For catalytic reactions levulinic acid and polyols e.g., trimethylolpropane (TMP) and pentaerythritol (PE), were also obtained from Merck.

2.2 Physical Measurements

Infrared spectroscopy (IR) analyses were scanned at the range of 4000-400 cm^{-1} with pressed KBr pellets using an IR-8400/8900 Shimadzu spectrophotometer. Magnetic susceptibility measurements were performed using a magnetic susceptibility balance (Sherwood Scientific, UK). The elemental analysis (carbon, hydrogen, and nitrogen) and metals were recorded by using a Yanaco CHN-corder-MT-5. The physical structure of catalysts, compositional analysis, and surface morphology observations were measured by scanning electron microscopy (SEM) (JEOL, JSM-6360 LV) coupled with energy-dispersive X-ray spectroscopy (EDS) (JEOL, JED-2300). The thermal decomposition behavior of residual hydrocarbons on the spent catalysts was carried out using thermogravimetric and differential thermal analysis (TGA/DTA 60, Shimadzu) at a heating rate of 10 $^{\circ}\text{C min}^{-1}$ from room temperature to 800 $^{\circ}\text{C}$ under nitrogen flow. Powder X-ray diffraction (XRD) analysis was performed using Rigaku RINT 2200 equipment with Cu-K α radiation operated at 40 kV and 40 mA. Data were collected over a 2 θ range of 10-90 $^{\circ}$ and phases were identified by matching experimental patterns to entries in the Version 6.0 indexing HighScore Plus software.

2.3 Synthesis of Metal Complexes

The syntheses of complexes (Scheme 1) were followed by the following reaction pathways where L-phenylalanine reacted with 4,4'-bipyridine, and/or L-tyrosine at 70-80 $^{\circ}\text{C}$ when metal salts were mixed with them and stirred for 2 h:



Scheme 1: The proposed reaction pathways for synthesizing complexes

2.3.1 Synthesis of $[\text{Ni}(\text{Phe})(\text{Bpy})\text{Cl}]\cdot\text{H}_2\text{O}$ (1)

Complex **1** was prepared with water:methanol (1:3) solution of L-phenylalanine (Phe) (1 mmol) and 4,4'-bipyridine (Bpy) [45] (1 mmol) which was previously deprotonated by alkali (NaOH, 0.05 mmol), to the nickel(II) chloride (1 mmol) solution, and continuously stirred at 60-70 $^{\circ}\text{C}$ for 2 h. Then, the cooled solution was filtered and the filtrate was placed at room temperature for slow evaporation of the solvent for crystallization. The powdered compound was collected and suitable for X-ray diffraction. Elemental analysis for $\text{C}_{19}\text{H}_{21}\text{N}_3\text{O}_3\text{ClNi}$, Calc. C: 52.71, H: 4.85, N: 9.71, Ni: 13.57, Found; C: 52.76, H: 4.90, N: 9.77, Ni: 13.64 %. Selected IR data (KBr pellet, cm^{-1}): 3310, 3149, 3123, 2937, 1601, 1348, 1565, 1437, 1350, 1231, 1077, 538, and 486. Magnetic susceptibility; $\mu_{\text{eff}} = 3.78$.

2.3.2 Synthesis of [Co(Phe)(Bpy)Cl].H₂O (2)

This complex was synthesized by applying the same procedure for **1**, repeating L-phenylalanine and 4,4'-bipyridine [45] as ligands, while substituting Ni(II) metal center with Co(II). The pink colored compound was obtained by slow evaporation of the concentrated solution and taken for powder X-ray diffraction. Elemental analysis for C₁₉H₂₁N₃O₃ClCo, Calc. C: 52.68, H: 4.85, N: 9.70, Co: 13.61, Found; C: 52.74, H: 4.89, N: 9.75, Co: 13.67 %. Selected IR data (KBr pellet, cm⁻¹): 3308, 3137, 2889, 1634, 1361, 1438, 1312, 1151, 1012, 596, and 475. Magnetic susceptibility; $\mu_{\text{eff}} = 4.65$

2.3.3 Synthesis of [Fe(Phe)(Tyr)Cl].H₂O (3)

The complex **3** was also prepared by employing the same procedure for complex **1**, using L-phenylalanine and L-tyrosine (Tyr) as ligands [46,47], and iron(II) chloride as metal salts. The greenish powdered compound was obtained by the slow evaporation of solvent which was suitable for powder X-ray diffraction studies. Elemental analysis for C₁₈H₂₄N₂O₆ClFe, Calc. C: 47.61, H: 5.29, N: 6.18, Fe: 12.30, Found; C: 47.66, H: 5.34, N: 6.24, Fe: 12.37 %. Selected IR data (KBr pellet, cm⁻¹): 3317, 3322, 3139, 2941, 1592, 1356, 1568, 1445, 1347, 1242, 1053, 530, and 489. Magnetic susceptibility; $\mu_{\text{eff}} = 4.85$.

3 Experimental for Catalytic Activity

3.1 Esterification

The catalytic activity experiments were accomplished via the esterification of levulinic acid (LA) with polyols (i.e., TMP and PE) under reflux condition at reaction temperature of 110-130°C in a silicone oil bath. The activities of catalysts were measured by varying different parameters involved (e.g., reaction time, % of catalyst loading, and polyols to LA molar ratios). Prior to reactions, the complex catalysts were dried at 50-60°C for 6 h to remove moisture (if any). Preliminary studies using sulfuric acid as a homogeneous catalyst were performed to estimate the range of reaction conditions. Blank experiments were conducted to validate the activity of the catalyst complexes. The applied reaction conditions were such that there was no external mass transfer; hence, the experiments were conducted under the same kinetic regime. After completion of each run, the products were collected and analyzed by Gas Chromatography-Mass Spectrometer (GC-MS, Shimadzu-QP 5000) equipped with RTX-5-MS column (30 m × 0.25 mm × 0.25 μm) in split mode. The fraction peaks obtained from mass spectra were identified using the National Institute of Standards and Testing (NIST) library matching. Furthermore, the catalytic activity of the catalysts towards esterification (total product yield and product selectivity) was determined by comparing the peak area % of the obtained spectra. It is known that the GC-MS analyses do not provide an exact quantitative analytical result of the compounds. However, it is possible to compare the product yield and selectivity by comparing the peak areas since the chromatographic peak area of compounds is proportional to its quantity and the relative content of the product (Eq. (1) and Eq. (2)) [48,49]. In order to confirm the reproducibility of the results, the experiments were performed three times, where the average of the peak area and peak area % was calculated. The levulinic acid conversion (Conv.) and turnover number (TON) was calculated by Eq. (3) and Eq. (4).

$$\text{Product Yield (\%)} = \frac{\text{Total area of product} - \text{area of reactant}}{\text{Total area of product}} \times 100\% \quad (1)$$

$$\text{Product Selectivity (\%)} = \frac{\text{Area of desired product}}{\text{Total area of product}} \times 100\% \quad (2)$$

$$\text{Conversion rate} = [(\text{Initial number of moles of substrate} - \text{final number of moles of products}) / \text{initial number of moles of substrate}] \times 100\% \quad (3)$$

$$\text{TON} = [(\text{Conversion rate} \times \text{total number of moles of the substrate}) / \text{number of moles of metal complex / acid}] \quad (4)$$

3.2 Hydrogenation (Reduction)

The *in situ* catalytic hydrogenation (upgrading) of TMP and PE-levulinate esters were conducted via NaBH₄ in a closed round-bottomed flask at room temperature with mechanical stirring. The NaBH₄ reducing agent was added to the esterified products and refluxed about 2 h with magnetic stirring at 25°C. Before reaction, the flask was cleaned and properly dried at 60°C for 8 h, and N₂ was flowed (three times) to eliminate any traces of oxygen in the system. At the end of each reaction, the round-bottomed flask was cooled, and the gases were liberated (if any). The reduced ester products were purified to remove catalyst by washing with 50 mL methanol (three times) at room temperature, and sent for Gas Chromatography Mass Spectrometry (GC-MS) and FT-IR analysis (liquid state).

4 Results and Discussion

The complexes [Ni(Phe)(Bpy)Cl].H₂O, [Co(Phe)(Bpy)Cl].H₂O, and [Fe(Phe)(Tyr)Cl].H₂O were synthesized successfully the first time by reacting Ni(II), Co(II), and Fe(II) chlorides with aromatic bidentate ligands, i.e., L-phenylalanine, 4,4'-bipyridine, and L-tyrosine as mixed ligands in water-methanol solution at 70-80°C. The thermal stability, magnetic susceptibility, spectroscopic, and X-ray diffraction studies are described in the experimental part. All the analytical and spectroscopic features are based on the good judgement of six coordinated complexes [25,45,47,50] in all the cases. The relevant IR spectroscopic and Gas Chromatography Mass Spectrometric (GC-MS) analysis for ester products are interpreted herein.

4.1 IR Spectra Analysis

Fourier transform infrared spectra (FTIR) of complexes 1, 2, and 3 were recorded between 4000-400 cm⁻¹ as shown in Fig. 1. There are characteristic stretching frequencies at 3475-3460 cm⁻¹, indicating the presence of O-H vibration of the coordinated water molecules to the complexes. The absorption bands appearing between 3334-3306 cm⁻¹ indicated the stretching vibration for N-H bonds [51]. Absorption peaks in the range of 3115-3045 cm⁻¹ are assigned to the C-H stretching vibration in the benzene/pyridine rings, lower wavenumber than free C-H bonds. The weak absorption peaks observed at 2916-2823 cm⁻¹ are the characteristics of C-H stretching vibration for methylene (-CH₂-) groups [46,52] in the complexes. The peaks observed at 1575-1016 cm⁻¹ are attributed to the stretching vibrations for benzene and pyridine rings [45]. The bands at 1645-1592 cm⁻¹ and 1368-1349 cm⁻¹ are the evidentiary absorptions for asymmetric and symmetric stretching vibration for >C=O groups (carbonyl) from the amino acid ligands [52], lower frequency than free carboxylate groups, which indicated M-O bonding. The bands at about 498-475 cm⁻¹ and 595-531 cm⁻¹ are also attributed to M-N and M-O stretching frequency [53], respectively. The coordination mode of N_{Bpy} and N_{Phe} to Ni(II) and Co(II), and O_{Tyr} and O_{Phe} atoms to Fe(II) are the agreement with bands observed at 590-485 cm⁻¹ [25,50,54,55].

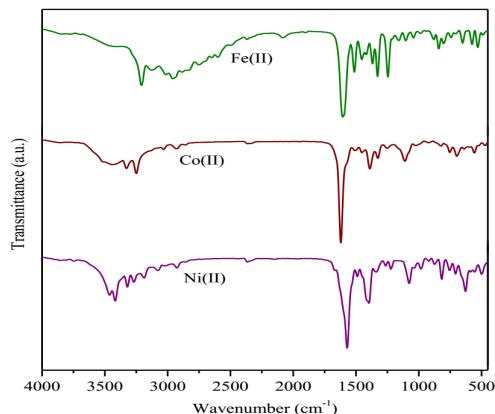


Figure 1: The FT-IR spectra of complexes 1, 2, and 3

4.2 Powder X-ray Diffraction Studies

The powder X-ray diffraction (XRD) analysis for [Ni(Phe)(Bpy)Cl].H₂O, [Co(Phe)(Bpy)Cl].H₂O, and [Fe(Phe)(Tyr)Cl].H₂O has been reported at the wavelength of 1.540598 Å (Fig. 2). The observed intensities vs. 2θ angles were collected from the transmission diffractogram of the finely powdered complexes. Moreover, the Miller indices h, k, and l values along with d-spacing were assigned to each 2θ angle. The results revealed that [Ni(Phe)(Bpy)Cl].H₂O belonged to the monoclinic crystal system [45], having unit cell parameters of a = 5.45, b = 10.75, and c = 11.35 Å; and α = 90, β = 112, and γ = 90°. For [Co(Phe)(Bpy)Cl].H₂O, results also implied monoclinic crystal system of unit cell parameters with a = 5.65, b = 10.65, c = 11.45 Å; and α = 90, β = 110, γ = 90°. For complex [Fe(Phe)(Tyr)Cl].H₂O, having same crystal system of unit cell parameters a = 5.55, b = 10.68, c = 11.48; and α = 90, β = 105, γ = 90 with maximum deviation of 2θ = 0.025° [56,57].

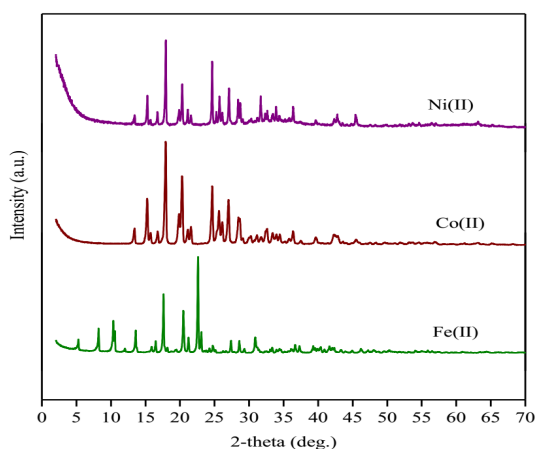
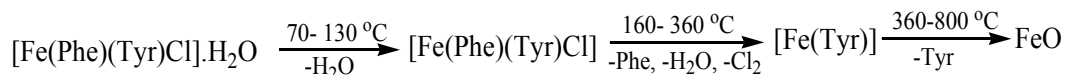
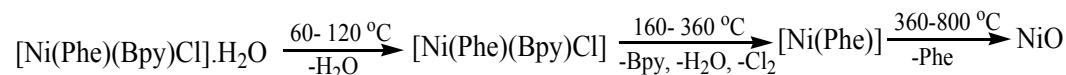


Figure 2: The Powder XRD pattern for complexes 1, 2, and 3

4.3 Thermogravimetric Analysis (TGA)

To interpret thermal stability of the complexes, the heating was suitably controlled at 10 °C min⁻¹ under inert N₂ atmosphere, and the weight loss was measured from the ambient temperature in between 60-800°C. The thermal fragmentation scheme for the complexes is shown below:



The Thermoanalytical data demonstrated that fragmentation occurred within 2-3 steps for the complexes (Tab. 1). The TGA curves (Fig. 3) revealed that the thermal decomposition takes place in the range of 60-130°C, 160-360°C, and 360-800°C. In the first step, endothermic fragmentation occurred at 60-130°C, where dehydration takes place. At the second step, endothermic decomposition between 160-360°C, eliminating coordinated water [58], chlorine and lower masses ligand molecules. At the third step, exothermic decomposition occurred between 360-800°C, whereby the remaining ligand molecules eliminating might leave behind the metal oxide (M₂O) as residue [25,59]. The ligand-metal complexes possibly follow a complicated degradative type pathway [60]. They might release Bpy ligand first, followed by Phe than Tyr ligand, leaving behind NiO, CoO, and FeO and the sequence of ligands

molecular masses are in the order of Bpy < Phe < Tyr [61]. Tab. 1 also described the details of weight loss upon decomposition.

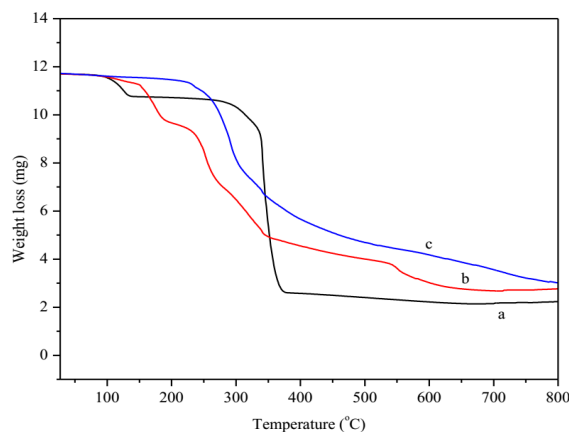


Figure 3: TGA curves of 1(a), 2(b), and 3(c) complexes under N₂ atmosphere

Table 1: Thermoanalytical data for 1, 2, and 3 complexes

Complexes	Temp. (°C)	TGA (wt. loss %)		Decomposition assignment
		Calc.	Found	
[Ni(Phe)(Bpy)Cl].H ₂ O (a)	60-120	4.16	6.73	Removal of one mole lattice H ₂ O molecule.
	160-360	48.47	45.28	Removal of one mole Bpy ligand, Cl ₂ and H ₂ O.
	360-800	82.50	82.20	Removal of one mole of Phe ligand.
[Co(Phe)(Bpy)Cl].H ₂ O (b)	70-130	4.15	3.38	Removal of one mole lattice H ₂ O molecule.
	160-360	48.44	43.18	Removal of one mole Bpy ligand, Cl ₂ and H ₂ O.
	360-800	82.47	77.96	Removal of one mole Phe ligand.
[Fe(Phe)(Tyr)Cl].H ₂ O (c)	70-130	3.97	-	Removal of one mole lattice H ₂ O molecule.
	160-360	48.19	41.44	Removal of one mole Phe ligand, Cl ₂ and H ₂ O.
	360-800	84.16	75.42	Removal of one mole Tyr ligand.

4.4 Scanning Electron Microscopy (SEM) Study

To study the surface morphology and physical structures of the catalysts, the scanning electron microscopy (SEM) analysis was performed. Fig. 4(a) and Fig. 4(b) revealed the presence of well-defined particles to the surface of transition metal complexes [62], while Fig. 4(c) showed agglomeration and non-uniformly dispersal of particles. It is obvious from the SEM images that all the synthesized metal complexes were assumed to have grown up just from a single molecule to several molecules in an aggregated distribution beginning from a few nanometres. Besides, different characteristic shapes of metal complexes were identified; these SEM images were quite different from other complexes. The SEM investigations checked the surfaces of the metal complexes that exhibited a small to medium particle, which have a tendency to agglomerate formation with different shapes analogous with the starting

materials [63]. In general, the SEM photograph displays a single phase formation with well-defined, grain-like shapes being particle sized in the range of $0.5\ \mu\text{m}$ [64]. In this context, the present investigation represents a unique pattern of a metal-organic framework assembly exhibiting that of a nanostructure. Moreover, we have envisaged the SEM micrographs of sample 1, 2, and 3 with a wide range of shapes and particle sizes to enhance the catalytic esterification [65], and hydrogenation.

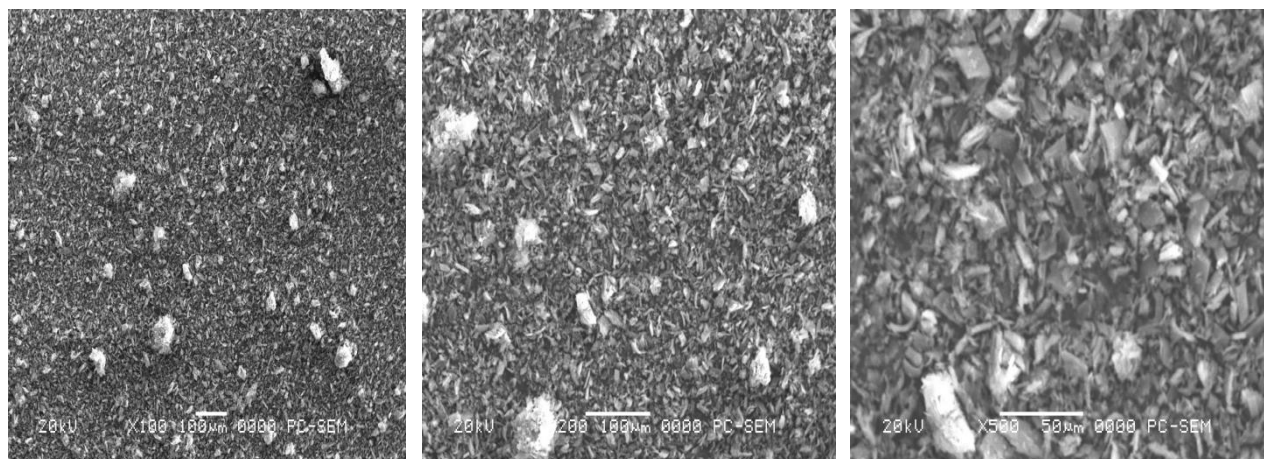


Figure 4(a): The SEM images of complex 1 at X100, X200 and X500 magnifications

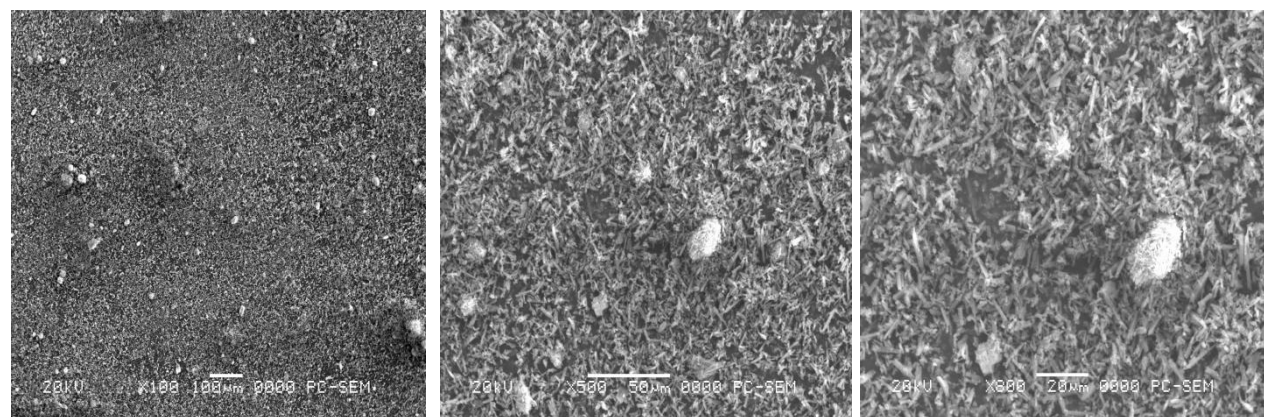


Figure 4(b): The SEM images of complex 2 at X100, X500 and X800 magnifications

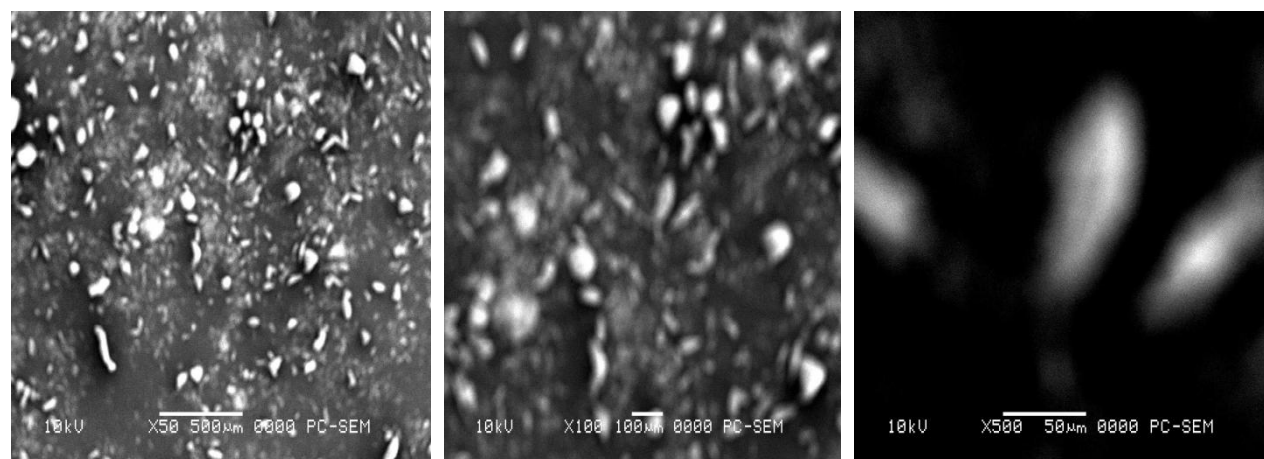


Figure 4(c): The SEM images of complex 3 at X50, X100 and X500 magnifications

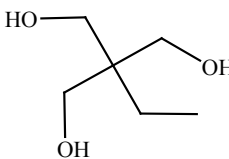
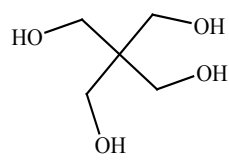
4.5 Catalytic Activity Study

4.5.1 Esterification

The catalytic activities of the complexes were measured via esterification reactions of levulinic acid (LA) with polyols, which are trimethylolpropane (TMP) and pentaerythritol (PE) (Tab. 2). Before examining the activity of complexes, preliminary studies using sulfuric acid as a liquid acid catalyst were conducted to estimate the range of reaction parameters (i.e., reaction time, catalyst loading, and polyols to LA molar ratios). Preliminary studies revealed that 51%-53% of LA + TMP esters, and 42%-43% of LA + PE esters were obtained with 2 wt.% catalyst loading of reaction time of 2 h. The molar ratio of LA to polyol was selected according to the stoichiometric ratio for the esterification reaction, where the molar ratio of LA:TMP was 3:1 and the molar ratio of LA:PE was 4:1. The reaction temperature was optimized at 115°C and 125°C for TMP and PE based on the ester yield and selectivity. A reaction time of 2 h and catalyst loading of 2 wt.% with respect to LA was optimized for all the complexes.

For all complexes, the esterification of LA with TMP gave higher yields compared to PE. The trimethylolpropane has three (-OH) groups, resulting to LA-mono, LA-di, and LA-tri esters. On the contrary, pentaerythritol having four alcoholic groups is less active, probably due to bulkiness of the molecule and a higher melting point (533 K), so no tetra-ester product [66] was detected in the course of study. To compare the catalytic performances of the complexes, similar reactions were conducted using H₂SO₄ as a catalyst [6], and found that metal complexes were more potential than H₂SO₄ as the selectivity was higher for di- and tri- esters.

Table 2: Esterification of levulinic acid with TMP and PE over Ni(II), Co(II), and Fe(II) complexes, H₂SO₄ and without catalyst

Polyols	Catalysts	Ester yield (%) ^b			LA conv. (mol%)	TON (h ⁻¹)
		Mono	Di	Tri		
 Trimethylolpropane ^a	[Ni(Phe)(Bpy)Cl]·H ₂ O	51.73	4.30	4.06	72.80	108
	[Co(Phe)(Bpy)Cl]·H ₂ O	53.14	5.93	3.03	76.50	111
	[Fe(Phe)(Tyr)Cl]·H ₂ O	57.01	7.11	6.13	78.70	113
	H ₂ SO ₄	51.00	3.00	1.50	40.20	103
	Blank experiment	14.86	2.00	0.85	18.25	0
 Pentaerythritol ^{a,c}	[Ni(Phe)(Bpy)Cl]·H ₂ O	45.71	7.40	5.21	70.25	105
	[Co(Phe)(Bpy)Cl]·H ₂ O	43.80	6.94	6.76	72.45	107
	[Fe(Phe)(Tyr)Cl]·H ₂ O	49.24	4.84	10.83	75.50	109
	H ₂ SO ₄	42.00	3.05	0.17	37.40	99
	Blank experiment	8.78	2.40	0.70	17.05	0

^aReaction conditions: Catalyst loading = 2% w/w of LA; LA: TMP = 3:1 at 115°C, LA: PE = 4:1 at 125°C; reaction time = 2 h.

^bCalculated using Eq. (1)

^cNo tetra-ester product was detected for PE

Turnover number (TON) = moles of LA converted per mole of total acidity of the catalyst per hour.

The present study also implies that the metal-organic coordination complexes are highly active for the esterification of LA with TMP and PE, producing significant amounts of levulinate-di and levulinate-tri esters. Furthermore, the catalytic reaction via esterification revealed that the most active homogenous catalyst is [Fe(Phe)(Tyr)Cl]·H₂O, which renders 70.25% LA + TMP with mono ester selectivity 60% and

(di + tri) ester selectivity of 34% followed by 64.91% for LA + PE with mono ester selectivity 51% and (di + tri) ester selectivity of 37%. Iron(II) is more Lewis acidic, due to the presence of more unpaired electron (d^6) than Co(II) and Ni(II).

4.5.2 Hydrogenation of (LA + TMP and LA + PE) Esters

The LA + TMP and LA + PE esters were further investigated for the *in situ* hydrogenation [67] with NaBH_4 in a round-bottomed flask (closed system) at room temperature for a two hour reflux. For hydrogenation, the molar ratio of LA:TMP: NaBH_4 was 3:1:0.5 and LA:PE: NaBH_4 was 4:1:0.5 [33,34]. The activity and selectivity of chemo- catalytic hydrogenation of LA + TMP and LA + PE esters to corresponding reduced esters over these catalysts (Tab. 3) is summarized. According to the esterification-hydrogenation reaction stoichiometry, one mole TMP/PE reacts with three/four moles LA, producing corresponding ester and reduced ester, respectively.

Hydrogenation (upgrading) of the levulinate esters is able to enhance its property as a biolubricant. Reduction of the ketone group in the levulinate chain was carried out by employing NaBH_4 in the presence of catalysts. Such reduction significantly reduces side reactions such as polymerization, which can happen with the elevated working temperature of lubricating systems.

The homogeneous catalysts were separated from the product by washing the product with cold methanol. The product was then heated at a low temperature of 65°C to evaporate the methanol, while the metal complexes were recovered via recrystallization.

Table 3: Hydrogenation of LA + TMP and LA + PE esters with NaBH_4 in the presence of Ni(II), Co(II), and Fe(II) complexes

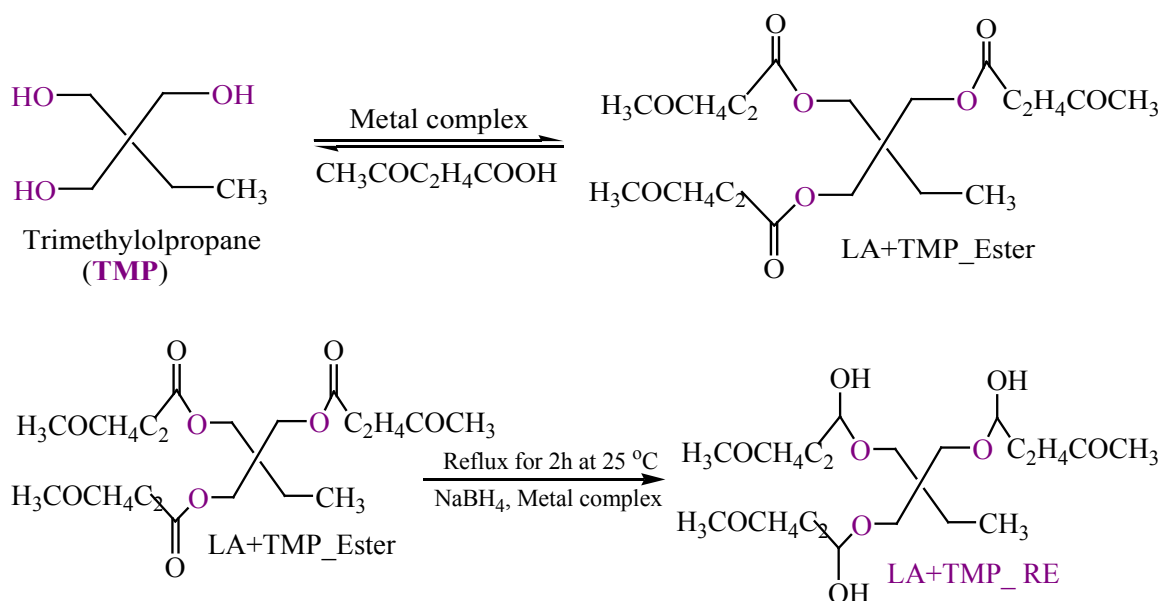
Ester type	Catalyst	Reaction type ^a	Reduced ester yield (%) ^b			LA conv. (mol%)	TON (h^{-1})
			Mono	Di	Tri		
LA + TMP	[Ni(Phe)(Bpy)Cl].H ₂ O	Reduction	49.78	4.13	3.85	68.80	101
LA + TMP	[Co(Phe)(Bpy)Cl].H ₂ O	Reduction	52.23	4.38	2.79	70.40	103
LA + TMP	[Fe(Phe)(Tyr)Cl].H ₂ O	Reduction	55.17	7.01	5.67	72.50	105
LA + PE	[Ni(Phe)(Bpy)Cl].H ₂ O	Reduction	44.76	6.58	4.92	65.30	99
LA + PE	[Co(Phe)(Bpy)Cl].H ₂ O	Reduction	43.23	5.43	6.45	67.20	100
LA + PE	[Fe(Phe)(Tyr)Cl].H ₂ O	Reduction	48.42	4.70	9.33	69.90	102

^aReaction conditions: Catalyst loading = 2% w/w of LA; LA: TMP: NaBH_4 = 3:1:0.5 at 25°C , LA: PE: NaBH_4 = 4:1:0.5 at 25°C ; reaction time = 2 h, product = reduced ester.

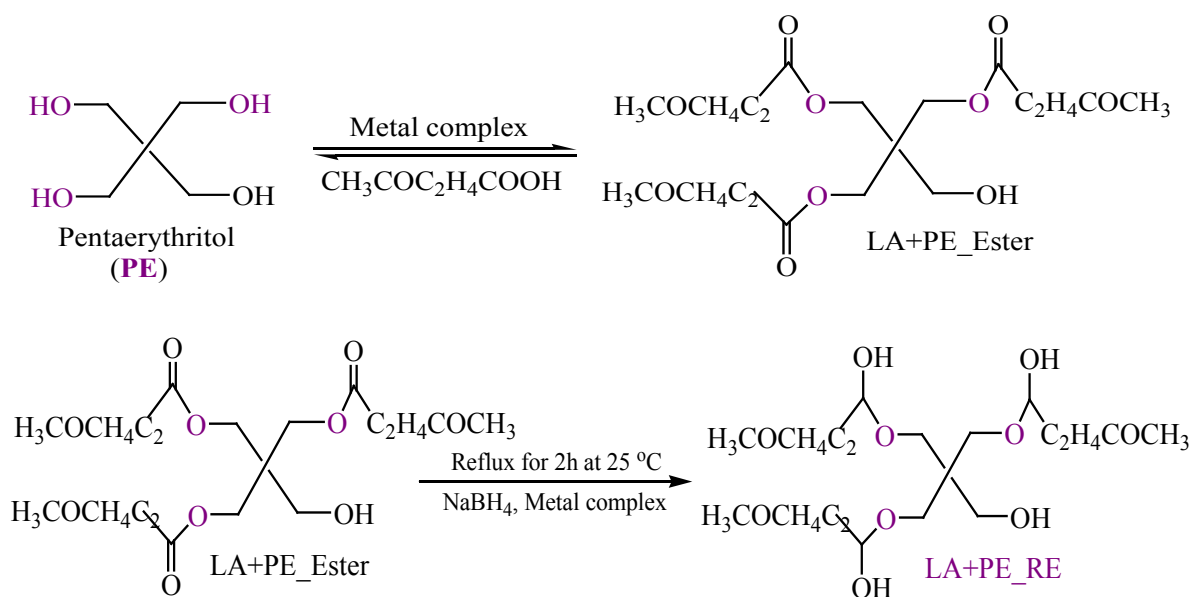
^bCalculated using Eq. (1)

Results from the experiment notified that the significant amounts of LA + TMP and LA + PE esters were reduced after hydrogenation. The reduction of LA + TMP and LA+PE esters was also absolutely confirmed based on the analysis of IR spectra. GC-MS analysis revealed that a maximum 67.85% reduced ester was isolated in the case of LA + TMP ester and 62.45% for LA + PE esters. Herein, [Fe(Phe)(Tyr)Cl].H₂O was an efficient catalyst for the hydrogenation of LA + TMP and LA + PE esters to corresponding reduced esters.

The route for synthesizing esters and reduced esters (Scheme 2 & Scheme 3) is as follows:

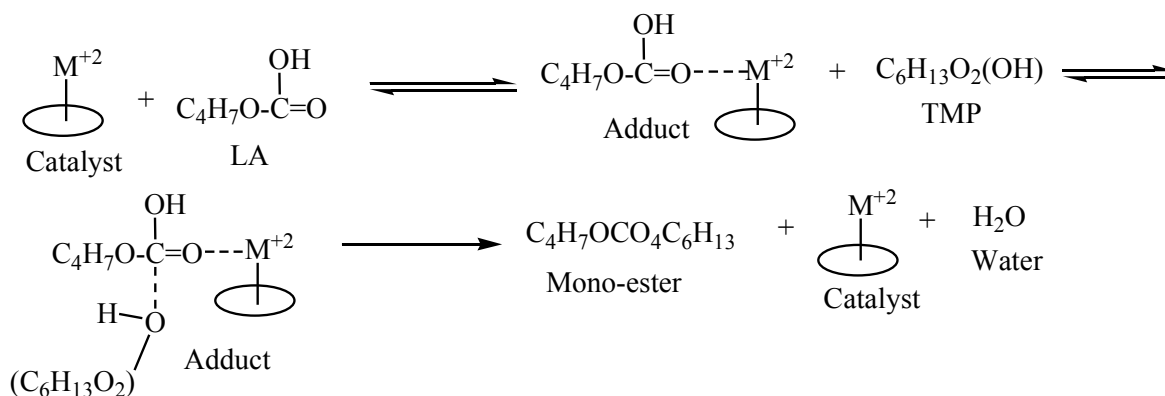


Scheme 2: Proposed schematic route for LA+TMP ester, and LA + TMP reduced ester



Scheme 3: Proposed schematic route for LA + PE ester, and LA + PE reduced ester

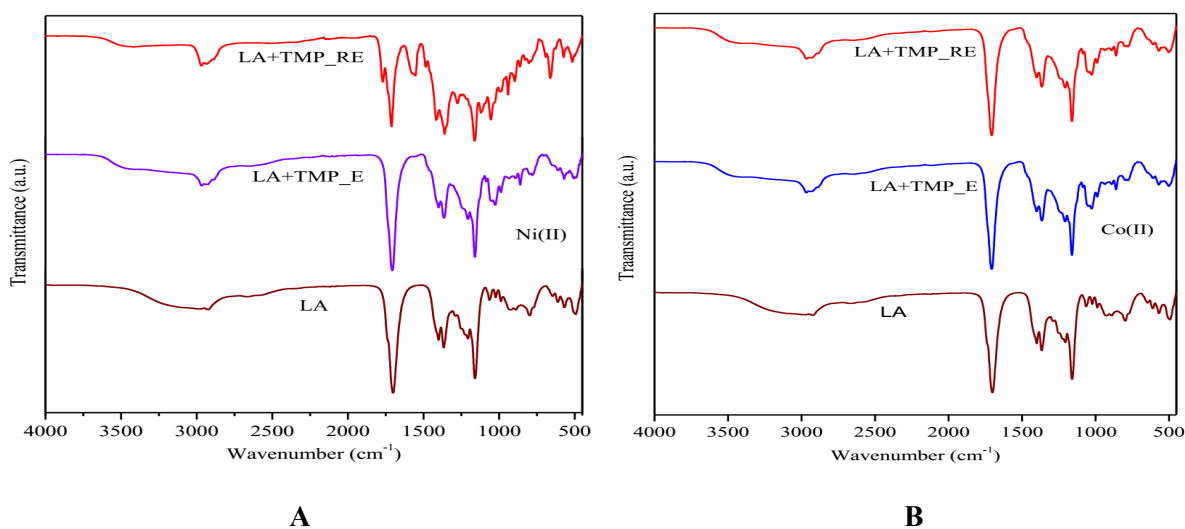
Levulinic acid (LA) reacts with polyols, i.e., trimethylolpropane (TMP) and pentaerythritol (PE), in the presence of acid catalyst to produce polyolesters. The reaction mechanism between levulinic acid and trimethylolpropane catalyzed by metal complexes for mono-esterification [68,69] was proposed. In general, Lewis acidity is associated with systems without protons, and the resulting catalytic activity is often attributed to interaction with catalyst metal cation [69]. Iron has d^6 electron system compared to cobalt (d^7) and nickel (d^8), resulting to more Lewis acidity when ionized, and produced higher amounts of ester. As shown in Scheme 4, the reaction involves the formation of an adduct between a carbonyl group and metal ion is as follows:

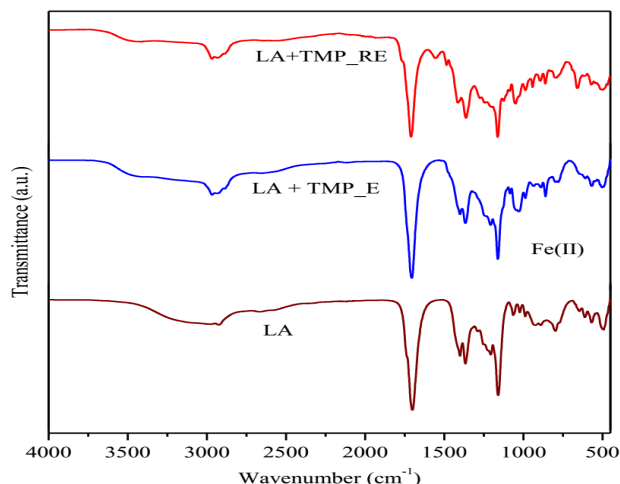


Scheme 4: Proposed mechanism of the mono-esterification between LA and TMP catalyzed by M^{+2}

4.5.3 IR Spectra Analysis for LA + TMP Reduced Ester

Fig. 5 demonstrates the FTIR spectrum (liquid state) for the ester product (E) and hydrogenated/reduced ester (RE) product, in comparison with pure levulinic acid. Pure levulinic acid (LA) showed four characteristic bands in the IR region, i.e., for C-H stretching at 2865 cm^{-1} (s), C=O stretching at 1710 cm^{-1} (s), C-O bending at 1165 cm^{-1} (s), and O-H stretching for carboxylic group at $3300\text{--}2800\text{ cm}^{-1}$ (b). After esterification with TMP, LA + TMP ester experienced a shift to a higher wavenumber for C-H vibration at $2880\text{--}2885\text{ cm}^{-1}$ (w), C-O bending at $1175\text{--}1178\text{ cm}^{-1}$ (w), and C=O stretching at $1723\text{--}1728\text{ cm}^{-1}$ (w) [70] for all complexes. The disappearance of O-H stretching frequency indicated that the -COOH groups from LA were converted into ester. After hydrogenation via NaBH_4 , the C=O stretching vibration appeared at $1733\text{--}1740\text{ cm}^{-1}$, and shifted about $10\text{--}12\text{ cm}^{-1}$ to a higher wavenumber for three complexes (Figs. 5(A), 5(B), and 5(C)) which undoubtedly indicated that ester groups were reduced.



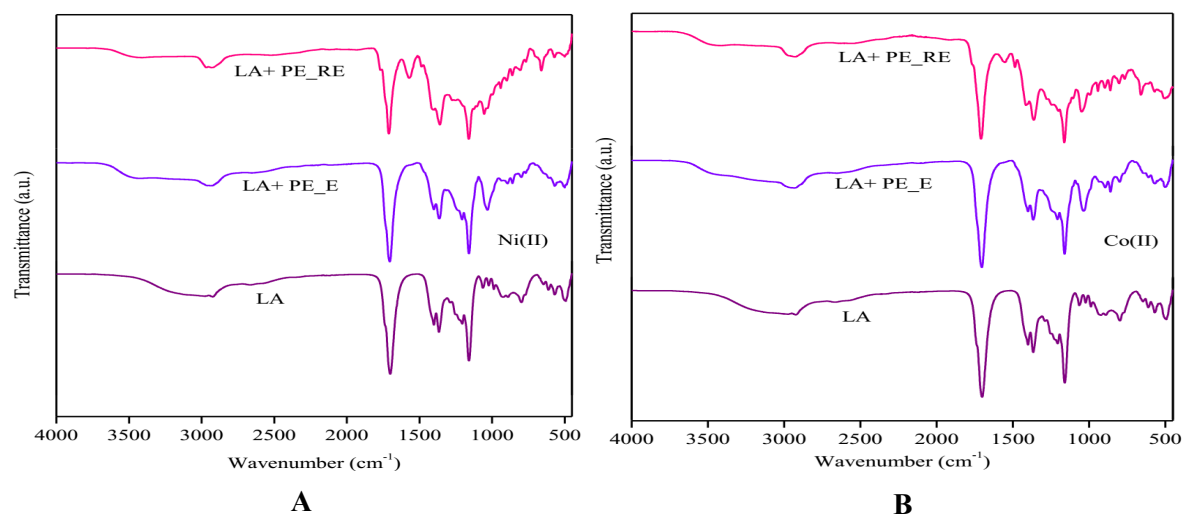


C

Figure 5: IR spectra of LA, LA + TMP_E, and LA + TMP_RE, respectively. By nickel(II) complex (A), cobalt(II) complex (B), and iron(II) complex (C)

4.5.4 IR Spectra Analysis for LA + PE Reduced Ester

Fig. 6 also represents the IR spectrum for the ester product and hydrogenated product, in comparison with levulinic acid (LA). The presence of ester groups and reduced esters are determined by the infrared spectrum (4000-400 cm⁻¹). Pure levulinic acid showed four characteristic bands in the IR region, i.e., for C-H stretching at 2865 cm⁻¹ (s), C=O stretching at 1710 cm⁻¹ (s), C-O bending at 1165 cm⁻¹ (s), and O-H stretching for carboxylic group at 3300-2800 cm⁻¹ (b). The ester product, LA + PE ester, exhibited characteristic bands to a higher wavenumber for C-H stretching vibration at 2885-2888 cm⁻¹ (w), C=O stretching at 1725-1728 cm⁻¹ (w), and C-O bending at 1178-1182 cm⁻¹ (w), which implied the formation of PE ester [71]. After hydrogenation, the C=O group experienced a little shift about 9-10 cm⁻¹ to a higher wavenumber at 1734-1738 cm⁻¹, while O-H stretching vibration disappeared (Figs. 6(A), 6(B), and 6(C)) for all complexes, which clearly indicated that ester groups were successfully reduced in their presence.



A

B

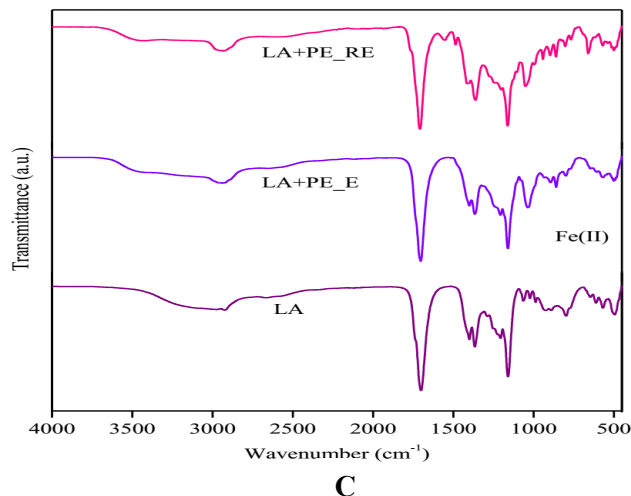


Figure 6: IR spectra of LA, LA + PE_E, and LA + PE_RE, respectively. By nickel(II) complex (A), cobalt(II) complex (B), and iron(II) complex (C)

5 Conclusion

We have synthesized two new polyol esters (i.e., LA + TMP and LA + PE ester) successfully using bio-oil model compound (levulinic acid) with the aid of metal complexes as catalyst. In the present study, biomass-derived bio-oil was considered as acid feedstock where levulinic acid was found as a major component. The polyol based-ester synthesized from non-food feedstocks via esterification, and upgrading through hydrogenation process has potential applications as lubricant base oil with the aid of blending and formulation method. The catalytic activities of the synthesized complexes were evaluated via esterification of levulinic acid with trimethylolpropane (TMP) and pentaerythritol (PE). Notably, the results indicated that the most active homogenous catalyst is $[\text{Fe}(\text{Phe})(\text{Tyr})\text{Cl}]\cdot\text{H}_2\text{O}$, which yields 70.25% LA+TMP and 64.91% LA + PE ester, respectively. Moreover, the catalysts were further examined for the *in situ* hydrogenation of levulinate esters, and GC-MS analysis revealed 67.85% reduced ester was isolated in the case of LA + TMP ester and 62.45% for LA+PE ester. The results among Ni(II), Co(II), Fe(II) complexes, Fe(II) was more active based on LA conversion and TON. Herein, it can be concluded that, six coordinated high spin (d^6) iron(II) complexes have higher catalytic activity in terms of all experimental results.

Acknowledgments: The authors acknowledge the financial support from Universiti Malaya (Grand Challenge (Innovative Technology (ITRC) (GC001B-14AET)), RU Geran (ST012-2018) and Postgraduate (Research Grant (PPP, Project number: PG250-2016A)).

References

1. Climent, M. J., Corma, A., Iborra, S. (2014). Conversion of biomass platform molecules into fuel additives and liquid hydrocarbon fuels. *Green Chemistry*, 16(2), 516-547.
2. Serrano-Ruiz, J. C., Luque, R., Sepulveda-Escribano, A. (2011). Transformations of biomass-derived platform molecules: from high added-value chemicals to fuels via aqueous-phase processing. *Chemical Society Reviews*, 40(11), 5266-5281.
3. Serrano-Ruiz, J. C., Pineda, A., Balu, A. M., Luque, R., Campelo, J. M. et al. (2012). Catalytic transformations of biomass-derived acids into advanced biofuels. *Catalysis Today*, 195(1), 162-168.
4. Bridgwater, A. V. (2012). Review of fast pyrolysis of biomass and product upgrading. *Biomass and Bioenergy*, 38, 68-94.

5. Gallezot, P. (2012). Conversion of biomass to selected chemical products. *Chemical Society Reviews*, 41(4), 1538-1558.
6. Ji, H., Wang, B. W., Zhang, X., Tan, T. W. (2015). Synthesis of levulinic acid-based polyol ester and its influence on tribological behavior as a potential lubricant. *RSC Advances*, 5(122), 100443-100451.
7. Oliveira, B. L., da Silva, V. T. (2014). Sulfonated carbon nanotubes as catalysts for the conversion of levulinic acid into ethyl levulinate. *Catalysis Today*, 234, 257-263.
8. Nandiwale, K. Y., Bokade, V. V. (2016). Optimization by Box-Behnken experimental design for synthesis of n-hexyl levulinate biolubricant over hierarchical H-ZSM-5: an effort towards agricultural waste minimization. *Process Safety and Environmental Protection*, 99, 159-166.
9. Hengne, A., Kadu, B. S., Biradar, N. S., Chikate, R. C., Rode, C. V. (2016). Transfer hydrogenation of biomass-derived levulinic acid to γ -valerolactone over supported Ni catalysts. *RSC Advances*, 6(64), 59753-59761.
10. Nandiwale, K. Y., Yadava, S. K., Bokade, V. V. (2014). Production of octyl levulinate biolubricant over modified H-ZSM-5: optimization by response surface methodology. *Journal of Energy Chemistry*, 23(4), 535-541.
11. Selva, M., Gottardo, M., Perosa, A. (2012). Upgrade of biomass-derived levulinic acid via Ru/C-catalyzed hydrogenation to γ -valerolactone in aqueous-organic-ionic liquids multiphase systems. *ACS Sustainable Chemistry & Engineering*, 1(1), 180-189.
12. Ortiz-Cervantes, C., Flores-Alamo, M., García, J. J. (2015). Hydrogenation of biomass-derived levulinic acid into γ -valerolactone catalyzed by palladium complexes. *ACS Catalysis*, 5(3), 1424-1431.
13. Ieda, N., Mantri, K., Miyata, Y., Ozaki, A., Komura, K. et al. (2008). Esterification of long-chain acids and alcohols catalyzed by ferric chloride hexahydrate. *Industrial & Engineering Chemistry Research*, 47(22), 8631-8638.
14. Cirujano, F. G., Corma, A., i Xamena, F. X. L. (2015). Conversion of levulinic acid into chemicals: synthesis of biomass derived levulinate esters over Zr-containing MOFs. *Chemical Engineering Science*, 124, 52-60.
15. Trombettoni, V., Bianchi, L., Zupanic, A., Porciello, A., Cuomo, M. et al. (2017). Efficient catalytic upgrading of levulinic acid into alkyl levulinates by resin-supported acids and flow reactors. *Catalysts*, 7(8), 235.
16. Hossain, M. A., Lqbal, M. A. M., Julkapli, N. M., Kong, P. S. (2018). Development of catalyst complexes for upgrading biomass into ester-based biolubricants for automotive applications: a review. *RSC Advances*, 8(10), 5559-5577.
17. Hossain, M. A., Lian, C. L. Y., Lslam, M. A. A. A. A., Sheikh, M. C., Ching, J. J. et al. (2018). Alumina-supported Cu (II), Co (II), and Fe (II) complexes as catalyst for esterification of biomass-derived levulinic acid with trimethylolpropane (TMP) and pentaerythritol (PE) and upgrading via hydrogenation. *BioResources*, 13(3), 5512-5533.
18. Choi, J., Choliy, Y., Zhang, X. W., Emge, T. J., Krogh-Jespersen, K. et al. (2009). Cleavage of SP³ C-O Bonds via Oxidative Addition of C-H Bonds. *Journal of the American Chemical Society*, 131(43), 15627-15629.
19. Huang, Z., Brookhart, M., Goldman, A. S., Kundu, S., Ray, A. et al. (2009). Highly active and recyclable heterogeneous iridium pincer catalysts for transfer dehydrogenation of alkanes. *Advanced Synthesis & Catalysis*, 351(1-2), 188-206.
20. Castonguay, A., Beauchamp, A. L., Zargarian, D. (2008). Preparation and reactivities of PCP-type pincer complexes of nickel. Impact of different ligand skeletons and phosphine substituents. *Organometallics*, 27(21), 5723-5732.
21. Goldman, A. S., Roy, A. H., Huang, Z., Ahuja, R. Schinski, W. et al. (2006). Catalytic alkane metathesis by tandem alkane dehydrogenation-olefin metathesis. *Science*, 312(5771), 257-261.
22. Muller, G., Klinga, M., Leskelä, M., Rieger, B. (2002). Iron and cobalt complexes of a series of tridentate P, N, P ligands-synthesis, characterization, and application in ethene polymerization reactions. *Zeitschrift für Anorganische und Allgemeine Chemie*, 628(13), 2839-2846.
23. Arashiba, K., Miyake, Y., Nishibayashi, Y. (2011). A molybdenum complex bearing PNP-type pincer ligands leads to the catalytic reduction of dinitrogen into ammonia. *Nature chemistry*, 3(2), 120-125.
24. Chakraborty, S., Krause, J. A., Guan, H. (2008). Hydrosilylation of aldehydes and ketones catalyzed by nickel PCP-pincer hydride complexes. *Organometallics*, 28(2), 582-586.

25. El-Behery, M., El-Twigry, H. (2007). Synthesis, magnetic, spectral, and antimicrobial studies of Cu(II), Ni(II) Co(II), Fe(III), and UO₂(II) complexes of a new Schiff base hydrazone derived from 7-chloro-4-hydrazinoquinoline. *Spectrochimica Acta Part A: Molecular and Biomolecular Spectroscopy*, 66(1), 28-36.
26. Morales-Morales, D., Jensen, C. G. (2010). *The chemistry of pincer compounds*. Elsevier.
27. Zhang, B., Lin, L., Zhuang, J., Liu, Y., Peng, L. et al. (2010). Hydrogenation of ethyl acetate to ethanol over Ni-based catalysts obtained from Ni/Al hydrotalcite-like compounds. *Molecules*, 15(8), 5139-5152.
28. Al Soom, N., Thiemann, T. (2016). Hydrogenation of alkenes with NaBH₄, CH₃CO₂H, Pd/C in the presence of O- and N-benzyl functions. *International Journal of Organic Chemistry*, 6(01), 1.
29. Yakabe, S., Hirano, M., Morimoto, T. (2000). Hydrogenation of alkenes with sodium borohydride and moist alumina catalyzed by nickel chloride. *Tetrahedron Letters*, 41(35), 6795-6798.
30. Satyanarayana, N., Periasamy, M. (1984). Hydroboration or hydrogenation of alkenes with CoCl₂-NaBH₄. *Tetrahedron letters*, 25(23), 2501-2504.
31. Suzuki, N., Kaneko, Y., Tsukanaka, T., Nomoto, T., Ayaguchi, Y. et al. (1985). Effective hydrogenation of carbon-carbon triple bonds by NaBH₄/PdCl₂ in polyethylene glycol/CH₂Cl₂: usefulness of peg in synthetic reactions. *Tetrahedron*, 41(12), 2387-2392.
32. Humphries, T. D., Kalantzopoulos, G. N., Llamas-Jansa, L., Olsen, J. E., Hauback, B. C. (2013). Reversible hydrogenation studies of NaBH₄ milled with Ni-containing additives. *The Journal of Physical Chemistry C*, 117(12), 6060-6065.
33. Saeed, A., Ashraf, Z. (2006). Sodium borohydride reduction of aromatic carboxylic acids via methyl esters. *Journal of Chemical Sciences*, 118(5), 419-423.
34. Boechat, N., da Costa, J. S. C., de Souza Mendonça, J., de Oliverira, P. S. M., de Souza, M. V. N. (2004). A simple reduction of methyl aromatic esters to alcohols using sodium borohydride-methanol system. *Tetrahedron letters*, 45(31), 6021-6022.
35. Chouhan, N., Ameta, R., Meena, R. K. (2017). Biogenic silver nanoparticles from *Trachyspermum ammi* (Ajwain) seeds extract for catalytic reduction of p-nitrophenol to p-aminophenol in excess of NaBH₄. *Journal of Molecular Liquids*, 230, 74-84.
36. Sun, W., Li, H., Wang, Y. (2015). Graphene-supported nickel chloride and cobalt chloride nanoparticles as highly efficient catalysts for dehydrogenation of ammonia borane. *International Journal of Hydrogen Energy*, 40(45), 15389-15397.
37. Kang, K., Gu, X., Liu, P., Sheng, X., Wu, Y. et al. (2015). Efficient catalytic hydrolytic dehydrogenation of ammonia borane over surfactant-free bimetallic nanoparticles immobilized on amine-functionalized carbon nanotubes. *International Journal of Hydrogen Energy*, 40(36), 12315-12324.
38. Feng, J., Yang, Z., Hse, S., Wang, K., Jiang, J. et al. (2017). In situ catalytic hydrogenation of model compounds and biomass-derived phenolic compounds for bio-oil upgrading. *Renewable Energy*, 105, 140-148.
39. Ashokraj, M., Mohan, V., Murali, K., Rao, M. V., Raju, B. D. (2018). Formic acid assisted hydrogenation of levulinic acid to γ -valerolactone over ordered mesoporous Cu/Fe₂O₃ catalyst prepared by hard template method. *Journal of Chemical Science*, 130, 16.
40. Kadam, H. K., Tilve, S. G. (2015). Advancement in methodologies for reduction of nitroarenes. *RSC Advances*, 5(101), 83391-83407.
41. Göksu, H. (2015). Recyclable aluminium oxy-hydroxide supported Pd nanoparticles for selective hydrogenation of nitro compounds via sodium borohydride hydrolysis. *New Journal of Chemistry*, 39(11), 8498-8504.
42. Wang, D., Astruc, D. (2015). The golden age of transfer hydrogenation. *Chemical Reviews*, 115(13), 6621-6686.
43. Nixon, T. D., Whittlesey, M. K., Williams, J. M. (2011). Ruthenium-catalysed transfer hydrogenation reactions with dimethylamine borane. *Tetrahedron Letters*, 52(49), 6652-6654.
44. Şen, F., Gökağaç, G. (2007). Activity of carbon-supported platinum nanoparticles toward methanol oxidation reaction: role of metal precursor and a new surfactant, tert-octanethiol. *Journal of Physical Chemistry C*, 111(3), 1467-1473.
45. Lu, J. Y., Lawandy, M. A., Li, J., Yuen, T., Lin, C. L. (1999). A new type of two-dimensional metal coordination systems: hydrothermal synthesis and properties of the first oxalate-bpy mixed-ligand framework

- [M (ox)(bpy)](M=Fe(II), Co(II), Ni(II), Zn(II); ox=C₂O₄²⁻; bpy=4, 4'-bipyridine). *Inorganic Chemistry*, 38(11), 2695-2704.
46. Hakimi, M., Aliabadi, T. S. (2012). Coordination chemistry of copper α -amino acid complexes. *Catena*, 6, 25.
 47. Lagaditis, P. O., Sues, P. E., Sonnenberg, J. F., Wan, K. Y. Lough, A. J. et al. (2014). Iron(II) complexes containing unsymmetrical P-N-P' pincer ligands for the catalytic asymmetric hydrogenation of ketones and imines. *Journal of the American Chemical Society*, 136(4), 1367-1380.
 48. El Khatib, S., Hanafi, S., Arief, M., Al-Amrousi, E. (2015). Hydrocracking of Jojoba Oil for green fuel production. *Journal of Petroleum Science and Technology*, 5(2), 59-69.
 49. Lian, C. L. Y., Voon, L. H., Hamid, S. B. A. (2017). Conversion of oleic acid model compound to biolubricant base oil using Al₂O₃ supported metal oxide catalyst. *Malaysian Journal of Catalysis*, 2(2), 46-52.
 50. Bauer, E. M., Cardarilli, D., Ercolani, C., Stuzhin, P. A., Russo, U. (1999). Tetrakis (thiadiazole) porphyrazines. 2. Metal Complexes with Mn(II), Fe(II), Co(II), Ni(II), and Zn(II). *Inorganic Chemistry*, 38(26), 6114-6120.
 51. Ismail, T. M. (2005). Mononuclear and binuclear Co(II), Ni(II), Cu(II), Zn(II) and Cd(II) complexes of Schiff-base ligands derived from 7-formyl-8-hydroxyquinoline and diamionaphthalenes. *Journal of Coordination Chemistry*, 58(2), 141-151.
 52. İnci, D., Aydin, R., Vatan, Ö., Yılmaz, D., Zorlu, Y. et al. (2017). Synthesis and crystal structures of novel copper(II) complexes with glycine and substituted phenanthrolines: reactivity towards DNA/BSA and *in vitro* cytotoxic and antimicrobial evaluation. *JBIC Journal of Biological Inorganic Chemistry*, 22(1), 61-85.
 53. Chandra, S., Kumar, U. (2005). Spectral and magnetic studies on manganese(II), cobalt(II) and nickel(II) complexes with Schiff bases. *Spectrochimica Acta Part A: Molecular and Biomolecular Spectroscopy*, 61(1), 219-224.
 54. Sanmartín, J., Bermejo, M. R., Garia-Deibe, A. M., Maneiro, M., Lage, C. et al. (2000). Mono- and polynuclear complexes of Fe(II), Co(II), Ni(II), Cu(II), Zn(II) and Cd(II) with N, N'-bis (3-hydroxysalicylidene)-1, 3-diamino-2-propanol. *Polyhedron*, 19(2), 185-192.
 55. Mohamed, G., Abd El-Wahab, Z. (2003). Salisaldehyde-2-aminobenzimidazole schiff base complexes of Fe(III), Co(II), Ni(II), Cu(II), Zn(II) and Cd(II). *Journal of thermal analysis and calorimetry*, 73(1), 347-359.
 56. Li, D., Xue, J., Ma, J., Tang, J. (2016). Synthesis of Fe₂(MoO₄)₃/MoO₃ heterostructured microrods and photocatalytic performances. *New Journal of Chemistry*, 40(4), 3330-3335.
 57. Puškarić, A., Halasz, I., Gredičak, M., Palčić, A., Bronić, J. (2016). Synthesis and structure characterization of zinc and cadmium dipeptide coordination polymers. *New Journal of Chemistry*, 40(5), 4252-4257.
 58. Dholariya, H.R., Patel, K. S., Patel, J. C., Patel, K. D. (2013). Dicoumarol complexes of Cu(II) based on 1, 10-phenanthroline: synthesis, X-ray diffraction studies, thermal behavior and biological evaluation. *Spectrochimica Acta Part A: Molecular and Biomolecular Spectroscopy*, 108, 319-328.
 59. Ikram, M., Rehman, S., Khan, A., Baker, R. J., Hofer, T. S. et al. (2015). Synthesis, characterization, antioxidant and selective xanthine oxidase inhibitory studies of transition metal complexes of novel amino acid bearing Schiff base ligand. *Inorganica Chimica Acta*, 428, 117-126.
 60. Asadi, Z., Asadi, M., Shorkaei, M. R. (2016). Synthesis, characterization and DFT study of new water-soluble aluminum(III), gallium(III) and indium(III) Schiff base complexes: effect of metal on the binding propensity with bovine serum albumin in water. *Journal of the Iranian Chemical Society*, 13(3), 429-442.
 61. Xing, N., Xu, L. T., Bai, F. Y., Shan, H., Xing, Y. H. et al. (2014). Synthesis and characterization of novel transition metal complexes with indole acetic acid ligands: evaluation of their catalytic activity for the oxidation of cyclohexane. *Inorganica Chimica Acta*, 409, 360-366.
 62. Khan, M., Khan, A., Hussain, I., Khan, M. A., Gul, S. et al. (2013). Spectral, XRD, SEM and biological properties of new mononuclear Schiff base transition metal complexes. *Inorganic Chemistry Communications*, 35, 104-109.
 63. Al-Saif, F. A. (2014). Spectroscopic elucidation, conductivity and activation Thermodynamic parameters studies on Pt(IV), Au(III) and Pd(II) 1, 5-dimethyl-2-phenyl-4-[(thiophen-2-ylmethylene)-amino]-1, 2-dihydro-pyrazol-3-one Schiff base complexes. *International Journal of Electrochemical Science*, 9, 398-417.

64. Anitha, C., Sheela, C. D., Tharmaraj, P., Shanmugakala, R. (2013). Studies on synthesis and spectral characterization of some transition metal complexes of azo-azomethine derivative of diaminomaleonitrile. *International Journal of Inorganic Chemistry*.
65. Boey, P. L., Ganesan, S., Maniam, G. P., Khairuddean, M., Efendi, J. (2013). A new heterogeneous acid catalyst for esterification: optimization using response surface methodology. *Energy Conversion and Management*, 65, 392-396.
66. Kotwal, M., Kumar, A., Darbha, S. (2013). Three-dimensional, mesoporous titanosilicates as catalysts for producing biodiesel and biolubricants. *Journal of Molecular Catalysis A: Chemical*, 377, 65-73.
67. Ji, T., Chen, L., Yuan, R. X., Knoblauch, M., Bao, F. S. et al. (2016). In-situ reduction of Ag nanoparticles on oxygenated mesoporous carbon fabric: exceptional catalyst for nitroaromatics reduction. *Applied Catalysis B: Environmental*, 182, 306-315.
68. Zeng, Z., Cui, L., Xue, W. L., Chen, J., Che, Y. (2012). Recent developments on the mechanism and kinetics of esterification reaction promoted by various catalysts. *Chemical kinetics*, pp. 255-282. InTech.
69. José da Silva, M., Lemos Cardoso, A. (2013). Heterogeneous tin catalysts applied to the esterification and transesterification reactions. *Journal of Catalysts*.
70. Arbain, N. H., Salimon, J. (2011). The effects of various acid catalyst on the esterification of Jatropha curcas oil based trimethylolpropane ester as biolubricant base stock. *Journal of Chemistry*, 8(S1), S33-S40.
71. Pavia, D., Lampman, G., Kriz, M. (2009). *GS introduction to spectroscopy*. Harcourt, Inc.: Florida, USA.